RESEARCH ARTICLE
July/August 2021 Volume 12 Issue 4 e01567-21
https://doi.org/10.1128/mBio.01567-21

Cysteine Mutants of the Major Facilitator Superfamily-Type Transporter CcoA Provide Insight into Copper Import

Bahia Khalfaoui-Hassani[a,b], Petru-Iulian Trasnea[a,*], Stefan Steimle[a], Hans-Georg Koch[c], and Fevzi Daldal[a]

[a]Department of Biology, University of Pennsylvaniagrid.25879.31, Philadelphia, Pennsylvania, USA
[b]Université de Pau et des Pays de l'Adour, E2S UPPA, IPREM, UMR CNRS 5254, Pau, France
[c]Institute of Biochemistry and Molecular Biology, ZBMZ, Faculty of Medicine, Albert Ludwigs University of Freiburg, Freiburg, Germany

ABSTRACT CcoA belongs to the widely distributed bacterial copper (Cu) importer subfamily CalT (CcoA-like Transporters) of the Major Facilitator Superfamily (MFS) and provides cytoplasmic Cu needed for *cbb*$_3$-type cytochrome *c* oxidase (*cbb*$_3$-Cox) biogenesis. Earlier studies have supported a 12-transmembrane helix (TMH) topology of CcoA with the well-conserved Met$_{233}$xxxMet$_{237}$ and His$_{261}$xxxMet$_{265}$ motifs in its TMH7 and TMH8, respectively. Of these residues, Met$_{233}$ and His$_{261}$ are essential for Cu uptake and *cbb*$_3$-Cox production, whereas Met$_{237}$ and Met$_{265}$ contribute partly to these processes. CcoA also contains five Cys residues of unknown role and, remarkably, its structural models predict that three of these are exposed to the highly oxidizing periplasm. Here, we first demonstrate that elimination of both Met$_{237}$ and Met$_{265}$ completely abolishes Cu uptake and *cbb*$_3$-Cox production, indicating that CcoA requires at least one of these two Met residues for activity. Second, using scanning mutagenesis to probe plausible metal-interacting Met, His, and Cys residues of CcoA, we found that the periplasm-exposed Cys$_{49}$ located at the end of TMH2, the Cys$_{247}$ on a surface loop between TMH7 and THM8, and the C$_{367}$ located at the end of TMH11 are important for CcoA function. Analyses of the single and double Cys mutants revealed the occurrence of a disulfide bond in CcoA *in vivo*, possibly related to conformational changes it undergoes during Cu import as MFS-type transporter. Our overall findings suggest a model linking Cu import for *cbb*$_3$-Cox biogenesis with a thiol:disulfide oxidoreduction step, advancing our understanding of the mechanisms of CcoA function.

IMPORTANCE Copper (Cu) is a redox-active micronutrient that is both essential and toxic. Its cellular homeostasis is critical for supporting cuproprotein maturation while avoiding excessive oxidative stress. The Cu importer CcoA is the prototype of the widespread CalT subfamily of the MFS-type transporters. Hence, understanding its molecular mechanism of function is significant. Here, we show that CcoA undergoes a thiol:disulfide oxidoreduction cycle, which is important for its Cu import activity.

KEYWORDS copper uptake, *cbb*$_3$-type cytochrome *c* oxidase, copper-binding residues, MFS-type transporters, *Rhodobacter capsulatus* CcoA, bacterial copper import, copper binding residues, *Rhodobacter capsulatus*, bacterial copper

homeostasis

Received 27 May 2021 **Accepted** 9 June 2021 **Published** 20 July 2021

* Present address: Petru-Iulian Trasnea, Institute of Science and Technology, Klosterneuburg, Austria.

Citation Khalfaoui-Hassani B, Trasnea P-I, Steimle S, Koch H-G, Daldal F. 2021. Cysteine mutants of the major facilitator superfamily-type transporter CcoA provide insight into copper import. mBio 12:e01567-21. https://doi.org/10.1128/mBio.01567-21.

Editor Gisela Storz, National Institute of Child Health and Human Development

The major facilitator superfamily (MFS) is one of the largest groups of secondary active transporters that are exceptionally diverse and ubiquitous to all three kingdoms of life. MFS members selectively transport a wide range of substrates, including sugars, amino acids, peptides, and antibiotics, either by utilizing the electrochemical gradient due to differential substrate concentration or by coupling the transport of one substrate to that of another via the so-called alternating-access mechanism (1, 2).

A typical MFS protein comprises 400 to 600 amino acids often arranged as 12 transmembrane α-helices (TMHs) in two pseudosymmetrical six N-terminal (N-ter) and six C-terminal (C-ter) TMH bundles, with both termini on the inner (*n*) side of the cytoplasmic membrane. In most cases, MFS proteins contain a substrate-binding cavity enclosed by the N- and C-ter domains and located about halfway into the membrane. The three-dimensional (3D) structures of several MFS transporters are available, and they exhibit different conformational states, supporting an alternating-access cycle mechanism of function (3–5). Accordingly, MFS-type transporters undergo a series of conformational changes to upload, and subsequently to release, their substrates across the membrane. These conformations are referred to as outward-open, outward-facing-occluded, inward-facing-occluded, and inward-open states. The interactions of the substrate with specific residues during its binding and its release are thought to trigger the dynamics of interdomain interactions (3, 6). The nature and location of the residues that selectively bind the substrate and those that trigger the conformational changes required for transport may differ among the MFS proteins. In the case of the lactose permease LacY, the residues TMH4-Glu_{126} and TMH5-Arg_{144} are essential for sugar binding, whereas the TMH7-Tyr_{236}, TMH8-Glu_{269}, and TMH10-His_{322}, which are close to one another in the inward-facing structure, coordinate the closing and the opening of the protein upon substrate binding and release (7, 8). For the oligopeptide transporter PepT, the residues TMH1-Tyr_{29}, TMH1-Tyr_{30}, and TMH2-Tyr_{68} are important for peptide binding, while TMH10-Gly_{407} and TMH11-Trp_{427} form the pivotal points that control the occluded and the inward-facing conformational states of PepT (9).

The MFS-type transporter CcoA was the first copper (Cu) importer reported in bacteria (10–12) and has become the prototype of the large CalT (CcoA-like Transporters) subfamily of Cu transporters (13). It was initially identified in the facultative phototroph *Rhodobacter capsulatus*, where it is required for the biogenesis of the binuclear heme-Cu (Cu_B) center of cbb_3-type cytochrome *c* oxidases (cbb_3-Cox) (14), a C family of heme-Cu O_2 reductase. Comparative phylogenomics of CcoA orthologs showed that they are widespread among the

alphaproteobacteria (15). In species like *Rhodobacter sphaeroides*, which produces multiple heme-Cu O_2 reductases, CcoA is specific to *cbb*$_3$-Cox and not involved in the maturation of the closely related *aa*$_3$-type Cox (15). This is noteworthy because both the *cbb*$_3$-Cox and *aa*$_3$-Cox have similar heme-Cu_B centers (16). Distant orthologs of *R. capsulatus* CcoA, initially thought to transport riboflavin, were shown to import Cu (13), and their occurrence in some proteobacteria lacking *cbb*$_3$-Cox suggests that CcoA-imported Cu is likely destined to other cuproproteins in these species. Thus, the CalT family members might have a broader role extending beyond the *cbb*$_3$-Cox biogenesis.

Previous studies addressing the Cu binding and import functions of CcoA revealed two motifs, $M_{233}xxxM_{237}$ and $H_{261}xxxM_{265}$, that are well conserved among its homologs (17). The membrane topology of CcoA and locations of these motifs in the predicted TMH7 and TMH8 suggested that they are parts of its membrane-buried Cu binding site (Fig. 1, left panel). Substitution of these residues with alanine, which is unable to ligand metals, and analyses of the ensuing mutants for ^{64}Cu uptake and *cbb*$_3$-Cox production had shown that the M_{233} and H_{261} residues are essential for CcoA activity, whereas substitution of M_{237}, or M_{265}, which are also parts of the conserved motifs, only partially affected the function (17). The putative Cu binding site of CcoA suggested that its mode of action was likely to be different from other well-studied eukaryotic Cu transporters, such as the Ctr-type (18) or the P-type (19) ATPase proteins.

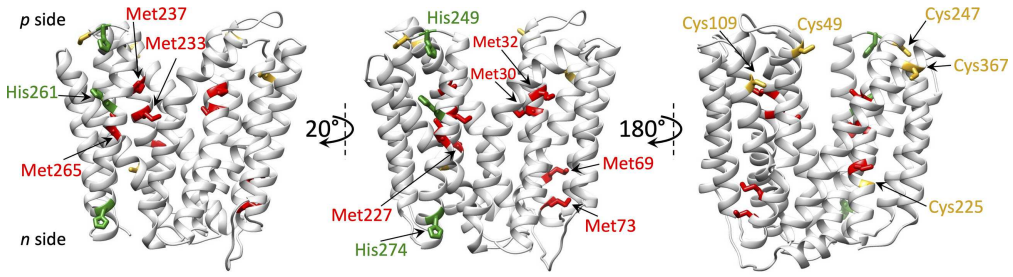

FIG 1 CcoA homology model using YajR as a template ($CcoA_{YajR}$) and locations of its selected Met, His, and Cys residues. Different views of $CcoA_{YajR}$ model generated using SWISS-MODEL (http://swissmodel.expasy.org; GMQE 0.51) are shown to highlight the respective locations of the conserved motifs ($M_{233}xxxM_{237}$ and $H_{261}xxxM_{265}$) proposed to bind Cu (left), the selected Met (M_{30}, M_{32}, M_{69}, M_{73}, and Met_{227}) and His (H_{249} and H_{274}) (middle), and the Cys (C_{49}, C_{109}, C_{225}, C_{247}, and C_{367}) (right) residues of CcoA examined in this study. The Met, His, and Cys residues are colored in red, green, and yellow, respectively.

Here, Cu import by *R. capsulatus* CcoA was studied in further detail. First, to better define the role of the M_{237} and M_{265} residues, a double mutant, $M_{237}A+M_{265}A$, was obtained and shown to be completely defective for Cu import and *cbb*$_3$-Cox activity, in contrast to the respective single mutants. In addition, the roles of selected five Met (M_{30}, M_{32}, M_{69}, M_{73}, and M_{227}), two His (H_{249} and H_{274}), and five Cys (C_{49}, C_{109}, C_{225}, C_{247}, and C_{367}) residues of CcoA (Fig. 1, middle and right panels) were examined by monitoring the *cbb*$_3$-Cox activities after mutagenesis. The results support a hypothetical model for *R. capsulatus* CcoA function, possibly involving thiol:disulfide exchange reactions between its periplasm-facing Cys residues during Cu import.

RESULTS

Either M_{237} or M_{265} residues of CcoA are required for Cu import. Earlier studies showed that mutants lacking CcoA were unable to accumulate ^{64}Cu in a

CcoA-specific (i.e., temperature-dependent) manner (12). Indeed, mutagenesis of the M_{233} and H_{261} residues of CcoA conserved motifs ($M_{233}XXXM_{237}$ and $H_{261}XXXM_{265}$) (Fig. 1, left panel) completely abolished *cbb*$_3$-Cox activity (Table 1), and cellular ^{64}Cu accumulation, while mutating M_{237} or M_{265} only partially decreased these activities (17). The results indicated that the conserved M_{233} and H_{261} residues of CcoA are essential for its function, likely forming its intramembrane Cu binding site. However, this study was less informative about the role(s) of the remaining M_{237} and M_{265} residues of the CcoA conserved motifs (17). To further pursue this issue, a double mutant ($M_{237}A+M_{265}A$) lacking both of these Met residues was obtained, and its properties were compared to the corresponding single mutants. Both *Escherichia coli* (Fig. 2A) and *R. capsulatus* (Fig. 2B) cells harboring the double mutant $M_{237}A+M_{265}A$ produced CcoA variant proteins at wild-type levels. The direct effects of these mutations on CcoA-dependent Cu uptake were determined by monitoring radioactive ^{64}Cu accumulation in whole cells (see Materials and Methods). Both *E. coli* and *R. capsulatus* cells producing this CcoA variant were deficient for ^{64}Cu uptake (Fig. 3A and B), similar to those mutants lacking CcoA. The *cbb*$_3$-Cox activity of the double mutant was also very low (~2% of wild type), in contrast to ~73% and ~35% of the single $M_{237}A$ and $M_{265}A$ mutants, respectively (Table 1). The *R. capsulatus* strain lacking a chromosomal copy of *ccoA* and complemented with a plasmid-borne wild type allele (*ΔccoA*/plasmid-born *ccoA*) (see Table S1 in the supplemental material) was used as a control and exhibited a *cbb*$_3$-Cox activity of 846 ± 32 μmol of tetramethyl-*p*-phenylenediamine (TMPD) oxidized/min/mg of total membrane proteins (referred to as 100% in Table 1). Considering that the CcoA variant lacking both M_{237} and M_{265} residues was unable to import Cu and produce active *cbb*$_3$-Cox, we concluded that at least one additional Met residue (preferentially M_{265}, suggested by its more severe phenotype) located three residues apart from the M_{233} or H_{261} on TMH7 or TMH8, respectively, is required for Cu import, probably as a Cu binding ligand.

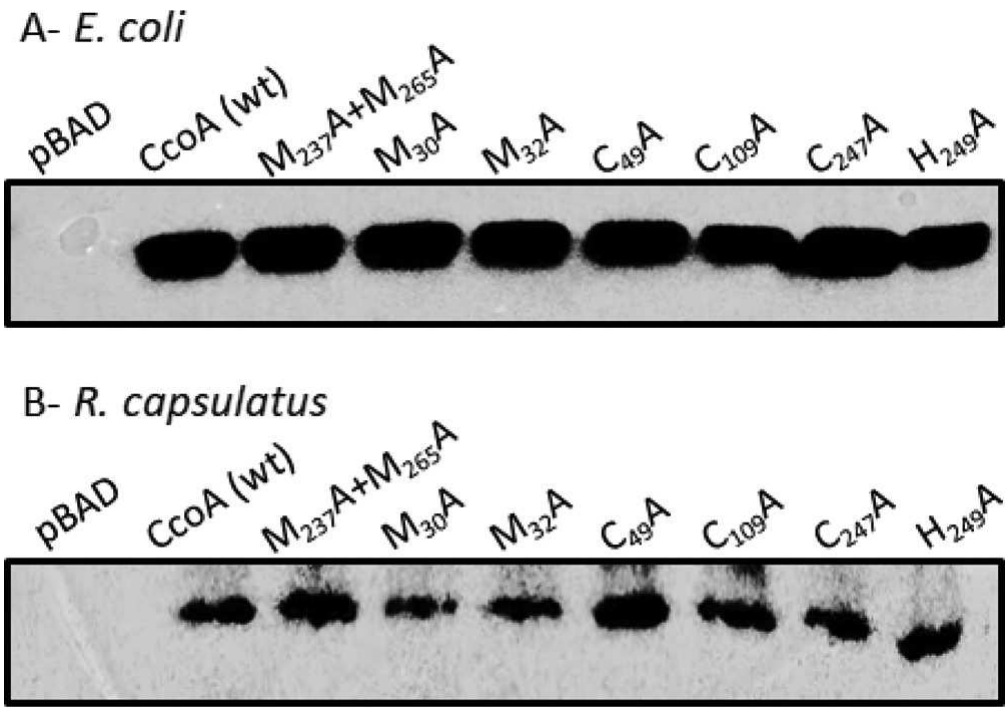

FIG 2 Production of mutant CcoA variants in *E. coli* and *R. capsulatus*. Membranes prepared from L-ara induced *E. coli* (LMG194) (A) and *R. capsulatus* Δ*ccoA* (SE8) (B) strains harboring appropriate plasmids (see Table S1) expressing wild-type or indicated CcoA mutant variants were probed with anti-Myc monoclonal antibodies. pBAD and CcoA (wt) correspond to

membranes prepared from *E. coli* (A) or *R. capsulatus* (B) strains harboring empty pBAD (*E. coli*) or pRK-pBAD (*R. capsulatus*) expression plasmids, and their derivatives containing Myc-tagged versions of wild-type and mutant *ccoA* alleles, as appropriate. All native and mutant proteins were produced adequately in both backgrounds.

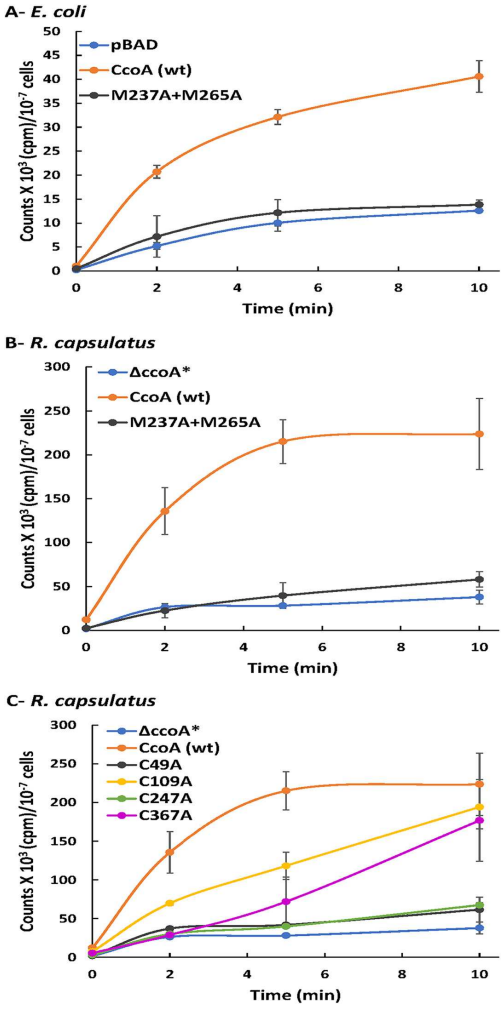

FIG 3 Whole-cell radioactive ^{64}Cu uptake by CcoA $M_{237}A$+$M_{265}A$ double and Cys single mutant derivatives. (A to C) ^{64}Cu uptake kinetics observed with the CcoA $M_{237}A$+$M_{265}A$ double mutant and $C_{49}A$, $C_{109}A$, $C_{247}A$, and $C_{367}A$ single mutants using appropriate L-ara induced *E. coli* (LMG194) (A) and *R. capsulatus* Δ*ccoA** (Δ*ccoA* Δ*copA*, SE24) (B and C) cells, expressing L-ara-inducible native and mutant *ccoA* alleles. pBAD and Δ*ccoA* refer to control strains, as appropriate. Uptake assays were performed as described in Materials and Methods. Activities measured in cells kept on ice were subtracted from those measured in cells incubated at 37°C, and assays were repeated at least three times using multiple independent cultures. CcoA (wt) refers to (Δ*ccoA*+plasmid-borne *ccoA*) strain carrying L-ara-inducible native CcoA, where Δ*ccoA** is Δ*ccoA* Δ*copA* (SE24), used to avoid frequent CopA revertants seen with a *ccoA* deletion (see Table S1) (12). Error bars correspond to the standard deviations around the mean values. In each case, at least three biological and three technical repeats were performed.

Strain	Residue location[b]	Conservation (%)[c]		cbb_3-Cox activity
		Rhodobacteriales	*Proteobacteria*	
Residues located in the conserved motifs of CcoA[a]				
Δ*ccoA/ccoA* (wt)*	NA[d]	NA	NA	100[e]
SE8 (Δ*ccoA*)*	NA	NA	NA	2
$M_{233}A$*	TMH7	100	100	9
$M_{237}A$*	TMH7	100	100	73
$H_{261}A$*	TMH8	100	100	3
$M_{265}A$*	TMH8	100	100	35
$M_{237}A+M_{265}A$	TMH7+THM8	100	100	2
Residues located elsewhere in CcoA				
$M_{30}A$	TMH1	90	10	78
$M_{32}A$	TMH1	80	0	72
$M_{69}A$	TMH2	0	0	88
$M_{73}A$	*n* side loop	100	60	29
$M_{227}A$	TMH7	50	20	75
$H_{249}A$	*p* side loop	10	40	87
$H_{274}A$	TMH8	90	30	71
$C_{49}A$	*p* end of TMH2	80	0	37
$C_{109}A$	*p* end of TMH4	0	70	75
$C_{225}A$	TMH7	100	20	70
$C_{247}A$	*p* side loop	100	50	6

$C_{367}A$	*p* end of TMH11	80	0	69

Additional possible metal-liganding CcoA residues of functional importance. CcoA is rich in Met, His, and Cys residues that can act as potential metal ligands (10), and those that are not parts of the conserved motifs were examined for their possible role(s). Two different amino acid sequence alignments were used with the proteobacterial homologs of CcoA that contributed to building the protein similarity network of the CalT subfamily (13). The *R. capsulatus* CcoA sequence was first aligned with its closely related CcoA homologs among the *Rhodobacterales* (mostly from node 1 [see reference 13]) (see Fig. S1). This comparison included *R. sphaeroides* CcoA known to provide Cu to *cbb*$_3$-Cox (16). The *R. capsulatus* CcoA sequence was also aligned with its more distant homologs among the different proteobacterial orders, including *Rhizobiales*, *Burkhorderiales*, *Pseudomonales*, *Rhodospirales*, *Vibrionales*, *Oceanospiralles*, *Synecchocales*, *Alteromonadales*, and *Chromatiales* (see Fig. S2). This group included *Ochrobactrum anthropi* (*Rhizobiales*) CalT (CcoA ortholog) shown to transport Cu (13) and possibly required for the maturation of cuproproteins distinct from *cbb*$_3$-Cox. Based on sequence alignments and topological locations (i.e., TMH or loop; Table 1) five Met (M_{30}, M_{32}, M_{69}, M_{73}, and M_{227}), possibly forming the M_{30}xM_{32} and M_{69}xxxM_{73} motifs (of which M_{30} and M_{73} are better conserved), two His (H_{249} and H_{274}), and five Cys (C_{49}, C_{109}, C_{225}, C_{249} and C_{367}) residues were retained for this study (Fig. 1, middle and right panels). They were substituted with Ala using L-ara-inducible *ccoA*, and the mutants obtained were introduced into appropriate *E. coli* and *R. capsulatus* strains (see Materials and Methods; Table S1). Their *cbb*$_3$-Cox and ^{64}Cu uptake activities were determined analogously to the conserved motifs mutants (17).

Properties of CcoA Met and His mutants. The CcoA single Met (M_{30}A, M_{32}A, M_{69}A, M_{73}A, and M_{227}A) mutants were produced in amounts similar to the wild type and M_{237}A+M_{265}A double mutant in both *E. coli* and *R. capsulatus* strains (Fig. 2, since the data are identical for all mutants tested, only M_{30}A and M_{32}A are shown). Of these residues, the M_{30}, M_{32}, M_{69}, and M_{73} form the so-called "Met (MxM and MxxxM) motifs," sometimes implicated in binding Cu(I) (20). The single M_{30}A, M_{32}A, and M_{69}A mutants on the N-ter domain and the M_{227}A single mutant located close to the M_{233}xxxM_{237} putative Cu binding motif on TMH7 had *cbb*$_3$-Cox activities slightly lower than that of wild-type CcoA (approximately 78, 72, 88, and 75% of wild-type amounts, respectively), similar to the single mutant M_{237}A (~73%) (Table 1). In contrast, mutating M_{73} that is located near the cytoplasmic end of TMH2 and highly conserved among the Rhodobacteriales CcoA homologs, led to a markedly lower c*bb*$_3$-Cox activity (~29%) like the single mutant M_{265}A (~35%) (Table 1) (17). The His_{249} and H_{274} are near the periplasmic and cytoplasmic (*p* and *n*) sides of the membrane, respectively, and only the latter residue is conserved in Rhodobacteriales (see Fig. S1). The corresponding mutants had *cbb*$_3$-Cox activities slightly lower than the wild type (ca. 87 and 71%, respectively) (Table 1). Thus, unlike M_{233} and H_{261}, none of these Met and His residues were required for CcoA function, except M_{73} located close to the cytoplasm, as its substitution significantly reduces *cbb*$_3$-Cox activity.

Properties of CcoA Cys mutants. Of the five Cys residues of CcoA, four (except C_{109}) are well-conserved especially among the Rhodobacteriales (see Fig. S1). Based on the homology model of CcoA ($CcoA_{YajR}$) obtained using its

highest homolog *E. coli* YajR (PDB 3WDO) as a template, the C_{49} and C_{367} residues are at or near the periplasmic ends of the TMH2 and TMH11, respectively, while C_{247} is located on a periplasmic loop between TMH7 and TMH8 (Fig. 1, right panel) (10, 17). The nonconserved C_{109} on TMH3, and the partly conserved C_{225} on TMH7 are more deeply embedded into the membrane, closer to the *p* and *n* sides, respectively. Substitution of each of these Cys residues with Ala did not affect the production of mutant proteins either in *E. coli* or *R. capsulatus* (Fig. 2; only C_{49}, C_{109}, and C_{247} are shown). However, it impaired the *cbb*$_3$-Cox activity of the mutant strains to different extents (Table 1). While the effects of C_{109}A, C_{225}A, and C_{367}A mutations were milder (ca. 75, 70, and ~69% of wild-type activity, respectively), those of the C_{49}A and C_{247}A were more severe (ca. 37 and ~6%, respectively). In respect to Cu import, upon L-arabinose (L-ara) addition radioactive ^{64}Cu accumulation in whole cells of a control strain lacking CcoA but harboring a plasmid-borne inducible CcoA (*ΔccoA*+plasmid-borne *ccoA*) steadily increased, unlike the *ΔccoA* strain lacking CcoA. With the C_{49}A or C_{247}A mutants, ^{64}Cu accumulation was very low, similar to the strain lacking CcoA, indicating that these residues are critical for CcoA function (Fig. 3C). On the other hand, the C_{109}A and C_{367}A mutants accumulated ^{64}Cu markedly more slowly to a slightly lower level than the control cells, indicating that C_{109} and C_{367} also contribute to Cu uptake but are not essential. Overall, the data indicated that these mutants fall into two groups (C_{49}A and C_{247}A versus C_{109}A and C_{367}A) with distinct kinetics behaviors, suggesting likely different functions.

Topological locations of periplasm-facing Cys residues of CcoA. Currently, no 3D structure of CcoA is available beyond the $CcoA_{YajR}$ homology model (Global Model Quality Estimate [GMQE] 0.51) based on its most pronounced homolog, which is the *E. coli* YajR (PDB 3WDO) (17). Fortunately, additional homology models of CcoA of similar GMQE yielding similar outcomes can be generated using available X-ray structures, including the iron exporter BpFPN (21). Here, we opted for two of its importer homologs, LacY (PDB 6C9W, $CcoA_{LacY}$, GMQE 0.46) and GlpT (PDB 1PW4, $CcoA_{GlpT}$, GMQE 0.44), captured in different conformations than $CcoA_{YajR}$. While an outward-open conformation (i.e., ready to receive the substrate from the *p* side of the membrane) is seen with $CcoA_{YajR}$, the $CcoA_{LacY}$ and $CcoA_{GlpT}$ models provide the occluded and the inward-open (i.e., ready to release the substrate to the *n* side of the membrane) conformations, respectively (Fig. 4A). Top views of these models clearly show that the distances separating the periplasm facing Cys residues change drastically depending on the conformations (Fig. 4B; see also Table S3, which lists all appropriate α-C-to-α-C distances). When $CcoA_{YajR}$ is in the outward-open conformation (Fig. 4B top), C_{49} and C_{109} located on the N-ter domain are very close to each other (C_{49}-C_{109}, 12 Å) and distant from C_{247} (C_{49}-C_{247}, 32 Å; C_{109}-C_{247}, 39 Å) and C_{367} (C_{49}-C_{367}, 22 Å; C_{109}-C_{367}, 32 Å) located on the C-ter domain. In the occluded conformation of $CcoA_{LacY}$ (Fig. 4B, middle), C_{49} moves closer to C_{247} (C_{49}-C_{247}, 23 Å) and C_{367} (C_{49}-C_{367}, 16 Å), while C_{109} shifts closer to both C_{247} and C_{367} (C_{109}-C_{247}, 36 Å; C_{109}-C_{367}, 28 Å). In the inward-open conformation of $CcoA_{GlpT}$ (Fig. 4B, bottom), C_{49} and C_{109} approach even closer to C_{247} (C_{49}-C_{247}, 16 Å; C_{109}-C_{247}, 27 Å) and C_{367} (C_{49}-C_{367}, 10 Å; C_{109}-C_{367}, 22 Å). In all conformations, the N-ter-located C_{49}-C_{109} pair stays within 12 to 14 Å, and the C-ter-located C_{247}-C_{367} pair remains within 19 to 22 Å of each other. Indeed, these distance estimations are approximations in the absence of 3D

structures. Nonetheless, they depict the progressive movement of the N-ter domain C_{49} toward the C-ter domain C_{247}-C_{367} pair during the transition from the outward-open to the inward-open conformations. This observation enticed us to inquire whether the predicted distance changes are related to the Cys residues that are exposed to the oxidizing periplasm undergoing thiol:disulfide oxidoreduction during CcoA function.

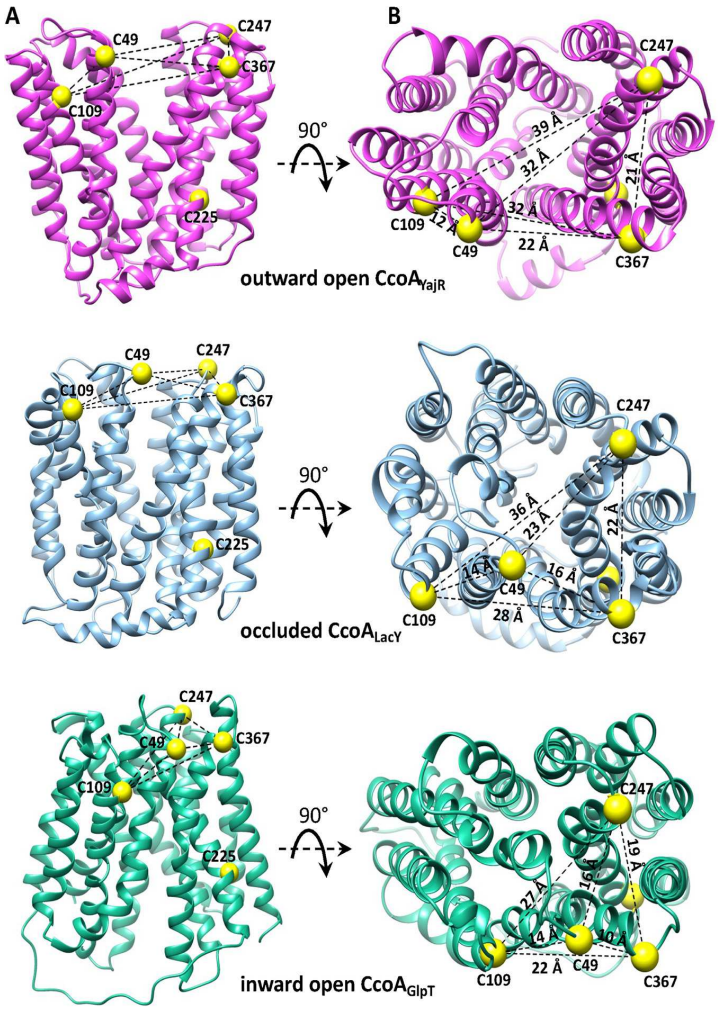

FIG 4 Different CcoA conformations and the distances that separate the periplasmic Cys residues in each conformational state. (A) Side views of *R. capsulatus* CcoA homology models ($CcoA_{YajR}$, $CcoA_{LacY}$, and $CcoA_{GlpT}$) representing its different conformations using as the templates *E. coli* YaJR (3WDO) in the outward-facing state (16% identity; GMQE 0.51), lactose permease LacY (1PV6) in the occluded state (12.7% identity; GMQE 0.41), and GlpT (1PW4) in the inward-facing state (11.7% identity; GMQE 0.46) (http://swissmodel.expasy.org). (B) Top views of the homology models shown in panel A, with the distances separating the periplasm-facing Cys residues (yellow balls) in different conformations of CcoA.

Disulfide bonds formed between the Cys residues of CcoA. The occurrence *in vivo* of disulfide bond(s) in CcoA was probed using *E. coli* cells expressing native CcoA or its Cys mutant variants and the thiol-reactive alkylating agent monomethyl-(PEG)24-maleimide (mPEG) (22). Alkylation of free Cys thiols of CcoA by mPEG is expected to increase its molecular weight (MW) by ~1.2 kDa per free thiol. In the case of disulfide bonds, alkylation occurs only after reduction by dithiothreitol (DTT), and then mPEG further increases the MW by ~2.4 kDa per reduced disulfide bond. The relative MW changes (M_r) in native and Cys mutant variants of CcoA were followed by SDS-PAGE/immunodetection (Fig. 5 and 6).

CcoA				CcoA Cys mutants				Identified -SH and -S~S-
-DTT		+DTT		-DTT		+DTT		
-mPEG	+mPEG	-mPEG	+mPEG	-mPEG	+mPEG	-mPEG	+mPEG	

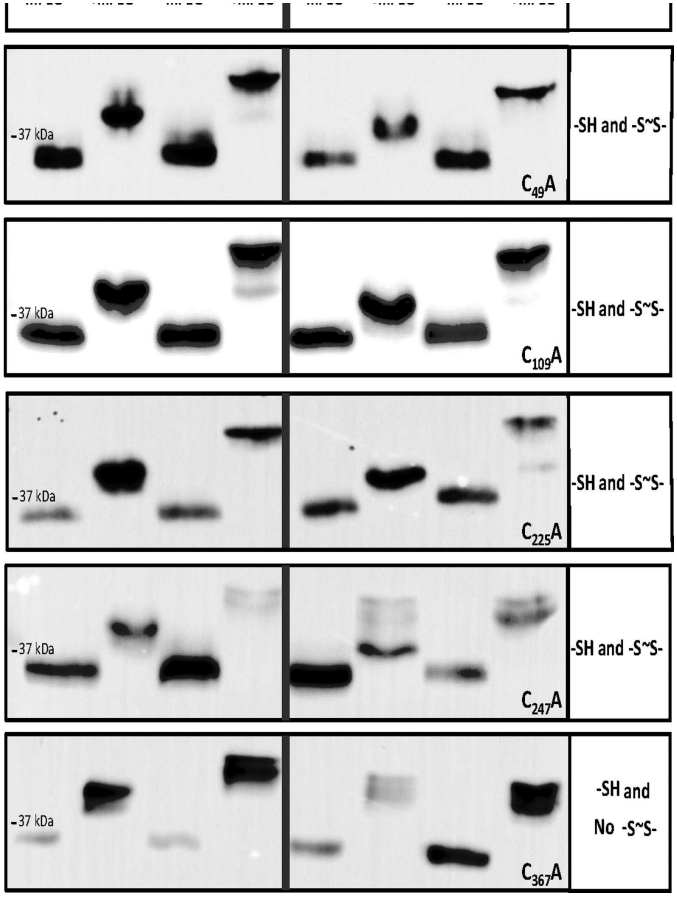

FIG 5 *In vivo* free thiols and disulfide bonds in native CcoA and its single Cys mutant derivatives. SDS-PAGE, followed by immunoblot analysis of *E. coli* cells expressing native and single $C_{49}A$, $C_{109}A$, $C_{225}A$, $C_{247}A$, and $C_{367}A$ mutant variants of CcoA. Cells growing in the presence of L-ara were treated mid-log phase for 10 min with or without DTT, followed by TCA precipitation and subsequent alkylation with or without mPEG. The presence of unmodified or mPEG alkylated CcoA was detected using anti-Myc monoclonal antibody and horseradish peroxidase conjugated anti-mouse IgG (see Materials and Methods). The total protein amounts of SDS-solubilized TCA-precipitated pellets could not be determined precisely, leading to variations of protein amounts loaded per lane. Thus, only the qualitive occurrence of M_r shifts in the absence or presence of DTT or mPEG were taken into consideration in this experiment.

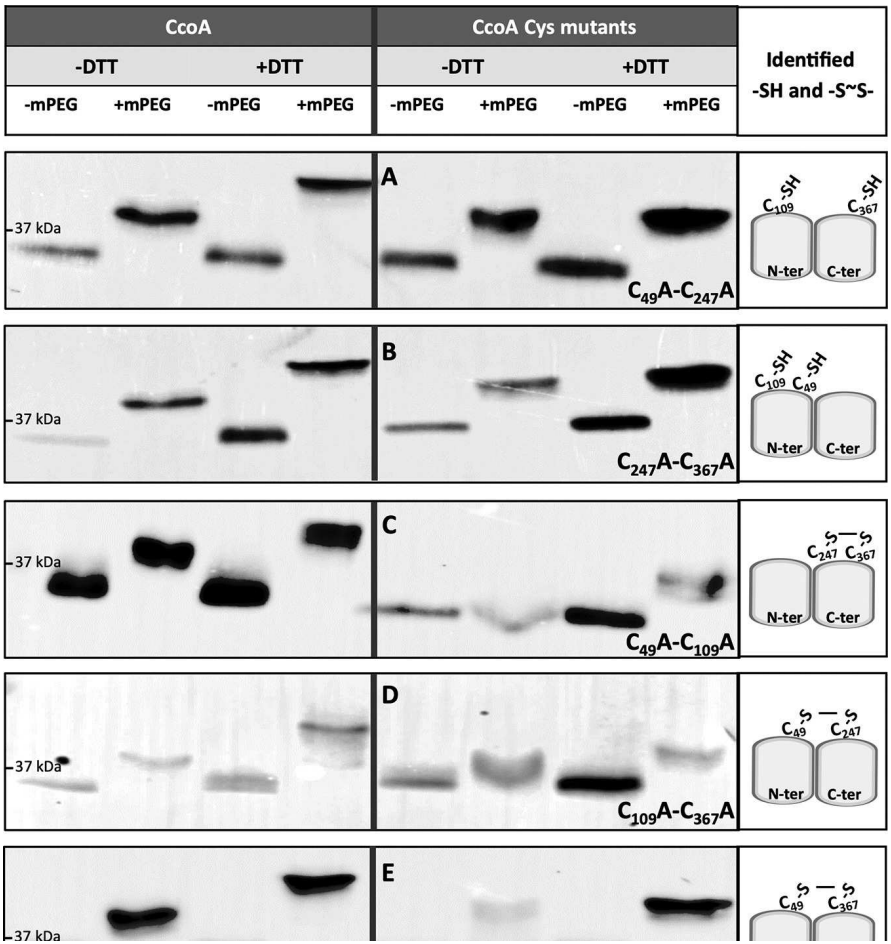

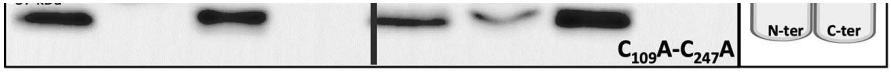

FIG 6 *In vivo* free thiols and disulfide bonds formed in native CcoA and its double Cys mutant derivatives. The experiments were conducted as described in Fig. 5, except that *E. coli* cells expressing the native (left side panels) and double mutant variants of CcoA were used: $C_{49}A$-$C_{247}A$ (A), $C_{247}A$-$C_{367}A$ (B), $C_{49}A$-$C_{109}A$ (C), $C_{109}A$-$C_{367}A$ (D), and $C_{109}A$-$C_{247}A$ (E). As in Fig. 5, the total protein amounts of SDS-solubilized TCA-precipitated pellets could not be determined precisely, leading to variations of protein amounts loaded per lane. Thus, only the M_r shifts detected in the absence or presence of DTT or mPEG were considered in these experiments.

Under our conditions, native CcoA (predicted MW of 37.4 kDa) runs as a band of ~35-kDa M_r in its oxidized or reduced forms (Fig. 5, left panels), which is not uncommon for membrane proteins. In the absence of DTT, alkylating by mPEG increased native CcoA M_r by ca. 3 to 4 kDa to ca. 38 to 39 kDa, suggesting that it contained three free Cys thiols (predicted M_r of 38.6 kDa after three mPEG addition). Moreover, alkylating native CcoA after DTT reduction further increased its M_r by another ~2-3 kDa to ca. 40 to 41 kDa, indicating that the native protein contained one disulfide bound *in vivo* (Fig. 5, left panels). Although detecting the ca. 1- to 2-kDa M_r differences with hydrophobic membrane proteins was challenging, following TCA precipitation all CcoA Cys residues appeared accessible to alkylation, including the Cys_{109} and Cys_{225}, which are more buried into the lipid bilayer according to the CcoA structural models (Fig. 1 and 4).

Similar mPEG alkylation experiments were repeated using single Cys mutant variants of CcoA (Fig. 5, right panels). Without DTT reduction, all single Cys mutant variants exhibited mPEG-induced M_r shifts similar to native CcoA, and the largest shift was seen with $C_{367}A$ mutant. In all cases but $C_{367}A$, the shifts were consistent with the likely presence of at least two free thiols, but not four as would have been expected upon elimination of any Cys residues already engaged in a disulfide bond in native CcoA. After DTT reduction, all single Cys mutants, except $C_{367}A$, showed the additional mPEG-induced M_r shifts, indicating that they still contained a disulfide bond formed among the remaining Cys residues. This observation suggested that native CcoA has more than two Cys residues that could form a disulfide bond(s). The $C_{367}A$ mutant was intensely alkylated but did not exhibit any readily detected mPEG-mediated M_r shift after DTT reduction, indicating that it contained no more disulfide bonds, and suggested that this residue provides one of the thiol groups forming a stable disulfide bond in native CcoA (Fig. 5, right panel, last row). Although occasionally additional minor bands were also seen in some cases (e.g., native CcoA, Fig. 5 left panel, second row, or $C_{225}A$, Fig. 5 right panel, third row), the data showed that the $C_{49}A$, $C_{109}A$, $C_{225}A$, or $C_{247}A$ single Cys mutants behaved similarly to each other and to native CcoA, which precluded identification of partner cysteines for forming a disulfide bond.

To identify the disulfide bond forming partner(s) in native CcoA *in vivo*, a set of double Cys mutants were examined (Fig. 6). All CcoA double Cys variants were produced adequately in *E. coli* and in *R. capsulatus* and exhibited low cbb_3-Cox activities like their cognate single Cys mutants. In the absence of DTT, mPEG alkylation data showed that the double mutants $C_{49}A$-$C_{247}A$ (with C_{109}, C_{225}, and C_{367} intact) and $C_{247}A$-$C_{367}A$ (with C_{49}, C_{109}, and C_{225} intact) had M_r shifts similar to each other, and to native CcoA, containing free thiols (Fig. 6A and B). However, like the C_{367} single mutant (Fig. 5, bottom row), these two double Cys mutants did not exhibit any additional mPEG-induced M_r increase upon reduction

by DTT, indicating that the remaining Cys residues did not form disulfide bonds. Conversely, the double mutants C_{49}-C_{109} (with C_{225}, C_{247}, and C_{367} intact) and C_{109}-C_{367} (with C_{49}, C_{225}, and C_{247} intact) showed no or slight mPEG-induced M_r shifts in the absence of DTT (although the absence of this shift was less clear in the latter double mutant) but exhibited clearer M_r shifts upon mPEG alkylation after DTT treatment (Fig. 6C and D). Since the C_{225} residue is near the *n* side and remote from the other periplasm-exposed Cys residues on the *p* side of the membrane, it is likely that in the C_{49}A-C_{109}A and C_{109}A-C_{367}A double mutants, the C_{247} and C_{367} and the C_{49} and C_{247} residues, respectively, formed disulfide bonds (although the latter pair might form a less stable disulfide bond) (Fig. 6C and D, far right). The slight M_r shifts seen with these double mutants in the absence of DTT reduction were consistent with the poor alkylation of C_{225}, still intact in these mutants. The remaining C_{109}A-C_{247}A double mutant (with C_{225}, C_{49}, and C_{367} intact) behaved essentially like the latter mutants, except that the CcoA population appeared heterogenous in the absence of DTT (Fig. 6E). A small fraction contained free thiols that was alkylated by mPEG without DTT treatment, whereas a large fraction contained a disulfide bond that could only be alkylated after DTT reduction. Again, assuming that C_{225} is too far from the other Cys residues to participate in disulfide bond formation, a large fraction of the C_{109}A-C_{247}A double-mutant population comprises a less stable disulfide bond between the C_{49} and C_{367} residues (Fig. 6E). In summary, the overall data indicated the formation of disulfide bonds between C_{49}~C_{247}, C_{49}~C_{367}, and C_{247}~C_{367} (with the last one forming the most stable bond) and the clear absence of disulfide bonds between C_{109}~C_{367} and C_{49}~C_{109}. This suggests that Cys_{109} is redox inactive, unlike the other periplasm-exposed residues, possibly due to its membrane-buried location in all conformations of CcoA (Fig. 4). Consequently, in cells producing native CcoA, any pair among the C_{49}, C_{247}, and C_{367} residues could form a single disulfide bond *in vivo*, leaving behind three free thiol groups, including C_{109} and C_{225}. This finding raised the possibility that native CcoA *in vivo* might exist as a heterogenous population with different conformations, presumably due to the import of spurious Cu presumably present in the growth medium. How the initial binding of Cu changes the conformation of CcoA and shuffles the free thiols and disulfide bonds between its three active Cys residues remains to be determined in future studies.

DISCUSSION

This study focused on the role of plausible metal-liganding residues Met, His and Cys of CcoA, a member of the CalT (CcoA-like Transporters) subfamily of MFS-type transporters (13) and the prototype of proteobacterial Cu importers (10, 15). The CalT subfamily is characterized by two well-conserved motifs (M_{233}xxxM_{237} and H_{261}xxxM_{265} in *R. capsulatus* CcoA) of which the first Met and His residues are absolutely required for Cu import (17). Here, we show that mutating concomitantly the M_{237} and M_{265} residues also abolishes CcoA activity, unlike the corresponding single mutants. Thus, the presence of at least one additional Met residue together with Met_{233} and His_{261} is required for Cu import. This finding further supports the Cu binding role of the conserved motifs that are the hallmark of the CalT subfamily of MFS-type transporters (13, 17).

We examined the distribution and topological location of additional possible metal-liganding residues of CcoA that are often conserved among its homologs, in particular those from the *Rhodobacterales* within the *Proteobacteria*. Of these

residues, mutating C_{225}, M_{227}, or H_{274} located at the TM7 and TM8 on the C-ter domain of CcoA near the membrane Cu-binding site, had little effect on CcoA activity. This finding was similar to that seen with the M_{237}A or M_{265}A single mutants, suggesting that they were either not critical for function, or partly substituted by surrogate residues. Intriguingly, mutating M_{73}, but not M_{69}, of the putative "Met" motif (M_{69}xxxM_{73} in *R. capsulatus*) (20) had a stronger effect on *cbb*$_3$-Cox activity. Homology models of the different conformations of CcoA do not seem to suggest that these N-ter residues come very close to the C-ter Cu binding residues. However, how Cu is released from CcoA is not yet known, leaving the possibility open that the C_{225}, M_{227}, and H_{274} residues or the putative Met (M_{69}xxxM_{73}) motif, or both, all positioned closer to the *n* side of the membrane, might play a role in this process.

Remarkably, mutating the periplasm-exposed C_{49}, C_{247}, and C_{367} residues affected CcoA activity to different degrees. These residues are well-conserved among the *Rhodobacterales*, but either less (~50% for C_{247}) or not (0% for C_{49} and C_{367}) conserved in other proteobacterial orders (see Fig. S1 and S2). The basis of this conservation is not obvious, but it might relate to the ultimate destination of Cu (e.g., *cbb*$_3$-Cox in *R. capsulatus* and other cuproenzymes in *O. anthropi*) and the different Cu donors and acceptors of CcoA and its homologs. Of the periplasm-facing Cys (C_{49}, C_{109}, C_{247}, and C_{367}) residues of CcoA, mutating C_{109} slowed Cu uptake (Fig. 3C), slightly affected *cbb*$_3$-Cox activity (Table 1), and mPEG alkylation indicated that C_{109} does not form a disulfide bond with either C_{367} or C_{49}. Intriguingly, C_{109} residue is not conserved among the *Rhodobacterales* (0%) but is better conserved (~70%) among the other orders of proteobacteria where CalT is thought to provide Cu to other cuproproteins distinct from the *cbb*$_3$-Cox (13).

Alkylation data of the single and double Cys mutants revealed that in native CcoA, two of the three periplasm-facing C_{49}, C_{247}, and C_{367} residues form a disulfide bond, while the remaining two remain as free thiol *in vivo*. Moreover, all possible disulfide and free thiol combinations among these residues (i.e., C_{247}~C_{367} leaving C_{49} free, C_{49}~C_{247} leaving C_{367} free, and C_{49}~C_{367} leaving C_{247} free) were observed in appropriate Cys double mutants. However, the levels of stability of these bonds seem to be different, with the C_{247}~C_{367} bond being most stable. Although the data in Fig. 6 tend to suggest that the C_{49}~C_{247} bond might be formed, yet the data with the single C_{367}A mutant (Fig. 5) suggest that it certainly must not be stable to be readily detected in this mutant. Assuming that CcoA undergoes conformational changes like any MFS-type transporter, the disulfide bond formation patterns suggest a hypothetical model linking Cu binding and conformational changes (Fig. 7). Accordingly, in the outward-open conformation of CcoA (state 1), C_{247} and C_{367} would contain a disulfide bond, far away from C_{49}. Binding of Cu would convert CcoA into its occluded conformation (state 2), bringing C_{49} near the C_{247}~C_{367} disulfide bond, and a nucleophilic attack would yield either C_{49}~C_{367} (Fig. 7, left) or C_{49}~C_{247} (Fig. 7, right) disulfide bond while freeing the remaining thiol of C_{247} or C_{367}. We note that if no such disulfide bond is formed or is extremely unstable, then the occluded conformation (state 2) may not have a disulfide bond (not shown in Fig. 7). In the exponentially growing cells used in this study, Cu import is not synchronized; thus, different conformations of CcoA must coexist, rendering impossible to discriminate between these possibilities at this stage. The more defective phenotype and the periplasmic

location (i.e., increased solvent exposure) of C_{247} as well as the weaker nature of C_{49}~C_{247} (as suggested by its absence in C_{367}A single mutant) and the detection of C_{49}~C_{367} (as seen with C_{109}A-C_{247}A double mutant) disulfide bonds might argue that the C_{49}-C_{367} disulfide bond may be more favorable at the inward open conformation (state 3) (Fig. 7, right). In any case, further progression of Cu within CcoA from the periplasm toward the cytoplasm would trigger the remaining free thiol (C_{247} or C_{367}) to attack the disulfide bond involving C_{49} (C_{49}~C_{247} or C_{49}~C_{367}) at the inward open conformation (state 3). The subsequent resolution of this bond would then reestablish the initial C_{247}~C_{367} disulfide bond and free C_{49} thiol, returning CcoA to its outward-open conformation (state 1). This model attributing more critical roles to C_{49} and C_{247} is also consistent with the highly defective ^{64}Cu uptake seen with the C_{49}A and C_{247}A single mutants (Fig. 3C). Conceivably, the three periplasm-facing C_{49}, C_{247}, and C_{367} residues that are highly conserved in Rhodobacterales may also play additional and perhaps different roles (e.g., liganding Cu) instead of those ascribed here. However, this hypothetical model suggests a link between the binding of Cu, ensuing conformation changes, and plausible thiol:disulfide oxidoreduction of CcoA. In this respect, the absence of *R. capsulatus* thiol: disulfide oxidoreductase DsbA (23), which catalyzes intramolecular disulfide bonds in extracytoplasmic proteins, is known to affect *cbb*$_3$-Cox biogenesis (24). Whether or not DsbA is involved in these thiol:disulfide exchange reactions seen with CcoA is presently unknown, but future studies addressing determination of the thiol:disulfide exchange reaction rates (e.g., using 5,5-dithio-bis-2-nitrobenzoic acid) (23) and the pKa values of appropriate thiols might identify the attacking and resolving Cys residues to further elucidate this process.

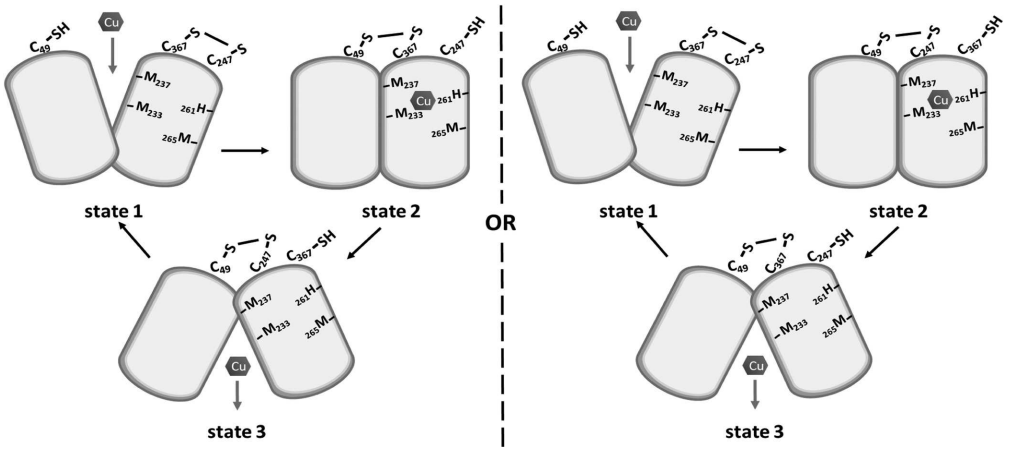

FIG 7 Hypothetical model linking substrate binding, conformational changes, and thiol:disulfide exchange reactions that CcoA might undergo during Cu import. Accordingly, at the onset CcoA has one disulfide C_{247}~C_{367} and C_{49}-SH (outward open state 1), binding of Cu induces a conformational change leading to occluded state 2, where a C_{49}~C_{367} (left side) or a C_{49}~C_{247} (right side) disulfide bond is formed (although the available data cannot rule out the absence of a disulfide bond at this state). Exchange of disulfide bonds and progress of Cu from the *p* to the *n* side of the membrane yield the inward open state 3. Upon release of Cu and resolution of the latter disulfide bond, CcoA is returned to its starting conformation.

Noticeably, other Cu transporters also have critical Cys residues. The Ctr-type transporters contain important Cys residues (within the HCH motif) at their C-terminal parts, near the *n* side of the membrane (25). They form disulfide bonds between the monomers of trimeric CTR1 to facilitate Cu release, unlike the periplasm-facing Cys residues of CcoA monomer, presumably involved in Cu uptake. Clearly, a requirement for Met, His, and Cys residues for CcoA activity

distinguishes its mechanism of function from other well-known Cu(I) transporters, including the eukaryotic Ctr1 (25–27) or the bacterial CopA and CusA (28, 29) proteins.

In summary, we showed here that the periplasm-facing Cys residues, together with the conserved membrane-embedded Cu-binding (M_{233}xxxM_{237}) and (H_{261}xxxM_{265}) motifs, are critical for proper function of the MFS-type Cu importer CcoA and possibly of its close homologs among Rhodobacterales.

MATERIALS AND METHODS

Growth conditions, strains, and plasmids used. The bacterial strains used in this work are described in Table S1 in the supplemental material. *Escherichia coli* strains were grown at 37°C on LB (lysogeny broth or Luria-Bertani) medium, supplemented with antibiotics (100 and 12.5 μg/ml ampicillin [Amp] and tetracycline [Tet], respectively) and L-arabinose (L-ara; 0.5%), as appropriate (17). The purple nonsulfur facultative photosynthetic *R. capsulatus* strains were grown at 35°C under respiratory (aerobic dark) conditions in enriched MPYE (minerals, bactopeptone, and yeast extract) medium supplemented with antibiotics (2.5 μg/ml Tet) and L-ara (0.5%), as needed (30).

Construction of CcoA mutants. Standard molecular genetic techniques were performed as described previously (31). The plasmids and primer sequences used are listed in Tables S1 and S2, respectively. The plasmid pBK68 carrying the L-ara-inducible *ccoA* is a derivative of pBAD/Myc-HisA (17) and used as a template for site-directed mutagenesis. Appropriate forward and reverse mutagenesis primers (see Table S2) were used to generate the plasmids pBK98 (M_{30}A), pBK99 (M_{32}A), pBK100 (M_{69}A), pBK101 (M_{73}A), pSP6 (M_{227}A), pSP4 (H_{249}A), pSP5 (H_{274}A), pBK108 (C_{49}A), pBK109 (C_{109}A), pSP9 (C_{225}A), pSP8 (C_{247}A), and pBK117 (C_{367}A), producing CcoA variants with the indicated mutations (see Table S1). These plasmids served as the templates for generating the *ccoA* double Met or Cys mutants by using appropriate forward and reverse primers (see Table S2) to yield pBK79 (M_{237}A+M_{265}A), pBK119 (C_{49}A+C_{109}A), pBK122 (C_{49}A+C_{247}A), pBK126 (C_{109}A+C_{247}A), pBK123 (C_{247}A+C_{367}A), and pBK129 (C_{109}A+C_{367}A), producing mutant CcoA variants (see Table S1). The pBAD derivatives carrying the mutant alleles of *ccoA* were cut with NsiI and ligated to the PstI site of the broad-host-range plasmid pRK415 to generate the following pBAD-pRK415 composite plasmid derivatives carrying the mutant *ccoA* alleles: pBK90 (H_{249}A), pBK95 (M_{237}A+M_{265}A), pBK102 (M_{30}A), pBK103 (M_{32}A), pBK104 (M_{69}A), pBK105 (M_{73}A), pBK92 (M_{227}A), pBK91 (H_{249}A), pBK111 (C_{49}A), pBK112 (C_{109}A), pBK94 (C_{225}A), pBK93 (C_{247}A), pBK120 (C_{367}A), pBK121 (C_{49}A+C_{109}A), pBK124 (C_{49}A+C_{247}A), pBK127 (C_{109}A+C_{247}A), pBK125 (C_{247}A+C_{367}A), and pBK130 (C_{109}A+C_{367}A) (see Table S1). These pRK derivatives were conjugated into appropriate *R. capsulatus* strains, as described earlier (17).

Chromatophore membrane preparation, SDS-PAGE, and immunodetection. Intracytoplasmic membrane vesicles (chromatophore membranes) were prepared in 20 mM Tris-HCl (pH 7.0) containing 150 mM NaCl and 1 mM phenylmethylsulfonylfluoride (PMSF) as previously described (30). Total protein concentrations were determined using the bicinchoninic acid assay (Sigma, Inc., procedure TPRO-562), and SDS-PAGE (12%) analyses were conducted as described previously (32). Prior to loading, 20 or 40 μg of proteins samples of *E. coli* or *R. capsulatus*, respectively, were solubilized by incubation at

room temperature for 10 min in a loading buffer (final concentration of 62.5 mM Tris-HCl [pH 6.8], 2% SDS, 2% β-mercaptoethanol, and 0.01% bromophenol blue). After electrophoresis, gels were electroblotted onto Immobilon-P polyvinylidene difluoride membranes (Millipore, Inc.), and probed with anti c-Myc tag monoclonal antibodies (clone 9E10 from the University of Pennsylvania Cell Center). The secondary antibodies were horseradish peroxidase-conjugated anti-mouse IgGs (GE Healthcare, Inc.), and the signal was detected using Supersignal West Pico chemiluminescence substrate according to the supplier's recommendations (Thermo Fisher, Inc.).

Determination of the free thiol groups and disulfide bonds of CcoA *in vivo*. *E. coli* cells producing wild-type or appropriate Cys mutant derivatives of CcoA were analyzed by alkylating free Cys thiols with methoxy-polyethylene glycol-maleimide (mPEG-MAL) before and after DTT reduction, as previously described (22). Strains producing desired CcoA variants were grown overnight at 37°C in 5 ml of LB medium supplemented with appropriate antibiotics (Amp, 100 μg/ml; Tet, 10 μg/ml) with shaking at 180 rpm. The next day,100 to 200 μl of these cultures were subcultured into 10 ml of fresh LB medium containing 1% L-ara and appropriate antibiotics at 37°C with shaking (180 rpm) until they reached an optical density at 600 nm (OD_{600}) of 0.5. At this stage, two aliquots of 0.9 ml each were taken out and kept on ice, while the remaining culture (8.2 ml) was reduced by addition of 82 μl of 1.0 M DTT (10 mM final concentration) and further incubated for 10 min at 37°C with shaking. Two additional aliquots of 0.9 ml each were taken and placed on ice. All four samples were precipitated by addition of 100 μl of 100% ice-cold TCA (final concentration, 10% [vol/vol]) and incubated on ice for 30 min. Precipitated materials were centrifuged at 13,000 rpm at 4°C for 12 min, and supernatants were removed without disturbing the pellets, which were washed with 300 μl of ice-cold acetone to eliminate TCA, and recentrifuged under the same conditions. The pellets were partially dried at 30°C for ~10 min to evaporate acetone, one untreated pellet and one DTT-treated pellet were resuspended in 30 μl of PBS buffer (137 mM NaCl, 2.7 mM KCl, 10 mM Na_2HPO_4, 2.0 mM KH_2PO_4 [pH 7.0]) supplemented with 0.1% SDS. Similarly, the remaining one untreated and one DTT-treated pellets were resuspended in 30 μl of mPEG-MAL solution (20 mM mPEG-MAL dissolved in PBS buffer) supplemented with 0.1% SDS. The pellets were vortexed vigorously for 1 min for complete dissolution, followed by incubation in the dark at room temperature for 2 h under constant shaking (1,000 rpm) to label the accessible thiol groups of CcoA. At the end of the incubation, 10 μl of 5× Laemmli buffer (10% SDS [vol/vol], 0.05% bromophenol blue [wt/vol], 60% glycerol [vol/vol], 300 mM Tris-HCl [pH 6.8]) was added to each sample, followed by further incubation at room temperature for 15 min. Then, 20 μl of each sample was loaded on a 12% nonreducing SDS-PAGE gel, run at 200 V, and subjected to immunoblot analyses using α-myc monoclonal antibodies (1:5,000 dilution) as primary antibodies and horseradish peroxidase conjugated anti-mouse IgGs as secondary antibodies (1:3,000 dilution). The addition of mPEG-MAL, specific to free thiol groups, increases the M_r of alkylated mPEG-MAL derivatives of CcoA, with the increases being proportional to the number of free thiol groups. Comparison of untreated and DTT-treated samples prior to mPEG-MAL alkylation visualized the DTT-reduced disulfide bonds of CcoA *in vivo* under the growth conditions used.

***cbb*$_3$-Cox activity.** The *in situ cbb*$_3$-Cox activity of *R. capsulatus* colonies was

assessed qualitatively using the "NADI" staining solution, which is made by mixing in a 1:1 (vol/vol) ratio 35 mM α-naphthol and 30 mM *N*,*N*,*N*′,*N*′-dimethyl-*p*-phenylene diamine (DMPD) dissolved in ethanol and water, respectively (33). Colonies producing cbb_3-Cox stain blue, while those lacking it remain unstained. The *in vitro* cbb_3-Cox activity was measured quantitatively using *R. capsulatus* chromatophore membranes and TMPD by monitoring spectrophotometrically in a stirred cuvette its oxidized form at 562 nm (λ_{562} = 11.7) at room temperature. Briefly, 10 µg of *R. capsulatus* chromatophore membranes was added to 1 ml of assay buffer (25 mM Tris-HCl [pH 7.0], 150 mM NaCl), and the enzymatic reaction was initiated by addition of TMPD at a final concentration of 1 mM. The TMPD oxidation specifically due to cbb_3-Cox activity was controlled by incubating the chromatophore membranes with 200 µM KCN for 2 min prior to TMPD addition. The cbb_3-Cox activity was calculated by subtracting from the TMPD oxidase activity the fraction that was KCN insensitive (15).

Radioactive ^{64}Cu uptake assays. Cellular Cu uptake assays were performed as previously described (12), using whole cells and radioactive ^{64}Cu (1.84×10^4 mCi/µmol specific activity) obtained from Mallinckrodt Institute of Radiology, Washington University Medical School. The. *E. coli* strains harboring appropriate pBAD/Myc-His derivatives with L-ara-inducible *ccoA* wild- type and mutant variants (see Table S1) were grown overnight in 10 ml of LB medium supplemented with 0.5% L-ara and appropriate antibiotics. Cells were pelleted, washed with the assay buffer (50 mM sodium citrate [pH 6.5], 5% glucose), and resuspended in 1 ml of the same buffer. All cultures were normalized to the same number of cells (7.5×10^8 cells/500 µl of assay volume) based on their absorbance (1 OD_{600} = 5×10^8 cells/ml for *E. coli* and 1 OD_{630} = 7.5×10^8 cells/ml for *R. capsulatus* strains). Cells to be assayed for ^{64}Cu uptake were preincubated at 35 or 0°C for 10 min before the assay. The uptake activity was initiated by addition of 10^7 cpm of ^{64}Cu, determined immediately before use (half-life of ^{64}Cu isotope ~12 h), and 50-µl aliquots were taken at 0, 1, 2, 5, and 10 min of incubation and immediately mixed with ice-cold 50 µl of 1 mM $CuCl_2$ and 50 µl of 50 mM EDTA (pH 6.5) to stop the uptake reaction. All aliquots were kept on ice until the end of the assay; the cells were then pelleted, and the pellets were washed twice with 100 µl of ice-cold 50 mM EDTA solution, resuspended in 1 ml of scintillation liquid, and counted using a scintillation counter (Coulter-Beckman, Inc.) with a wide-open window. For each time point, the background ^{64}Cu uptake activity seen at 0°C was subtracted from that at 35°C and plotted as a function of time to compare CcoA-specific Cu uptake of wild-type control (*ΔccoA*/plasmid-born *ccoA*) and mutant derivatives of CcoA.

NOTE

This article is a direct contribution from Fevzi Daldal, a Fellow of the American Academy of Microbiology, who arranged for and secured reviews by J. Beatty, University of British Columbia; Soufian Ouchane, French National Centre for Scientific Research; and Carsten Sanders, Kutztown University of Pennsylvania.

ACKNOWLEDGMENTS

This study was supported mainly by the Division of Chemical Sciences, Geosciences and Biosciences, Office of Basic Energy Sciences of Department of Energy (DOE DE-FG02-91ER20052) to F.D., partly by the National Institutes of Health (GM 38237) to F.D., and by the Deutsche Forschungsgemeinschaft (RTG 2202, Project-ID 278002225) to H.-G.K.

We declare that the research was conducted in the absence of any commercial or

financial relationships that could be construed as a potential conflict of interest.

All authors have given approval to the final version of the manuscript. B.K.-H., P.-I.T., and F.D. designed, performed experiments, and analyzed data. S.S. performed structural analyses, and all authors critically read and edited the manuscript. B.K.-H., H.-G.K., and F.D. supervised the study.

REFERENCES

1. Marger MD, Saier MH, Jr. 1993. A major superfamily of transmembrane facilitators that catalyse uniport, symport and antiport. *Trends Biochem Sci* 18:13–20. 10.1016/0968-0004(93)90081-W. PubMed.
2. Pao SS, Paulsen IT, Saier MH, Jr. 1998. Major facilitator superfamily. *Microbiol Mol Biol Rev* 62:1–34. 10.1128/MMBR.62.1.1-34.1998. PubMed.
3. Yan N. 2013. Structural advances for the major facilitator superfamily (MFS) transporters. *Trends Biochem Sci* 38:151–159. 10.1016/j.tibs.2013.01.003. PubMed.
4. Quistgaard EM, Low C, Guettou F, Nordlund P. 2016. Understanding transport by the major facilitator superfamily (MFS): structures pave the way. *Nat Rev Mol Cell Biol* 17:123–132. 10.1038/nrm.2015.25. PubMed.
5. Abramson J, Smirnova I, Kasho V, Verner G, Kaback HR, Iwata S. 2003. Structure and mechanism of the lactose permease of *Escherichia coli*. *Science* 301:610–615. 10.1126/science.1088196. PubMed.
6. Abramson J, Riistama S, Larsson G, Jasaitis A, Svensson-Ek M, Laakkonen L, Puustinen A, Iwata S, Wikstrom M. 2000. The structure of the ubiquinol oxidase from *Escherichia coli* and its ubiquinone binding site. *Nat Struct Biol* 7:910–917. 10.1038/82824. PubMed.
7. Abramson J, Smirnova I, Kasho V, Verner G, Iwata S, Kaback HR. 2003. The lactose permease of *Escherichia coli:* overall structure, the sugar-binding site and the alternating access model for transport. *FEBS Lett* 555:96–101. 10.1016/s0014-5793(03)01087-1. PubMed.
8. Zhou Y, Jiang X, Kaback HR. 2012. Role of the irreplaceable residues in the LacY alternating access mechanism. *Proc Natl Acad Sci U S A* 109:12438–12442. 10.1073/pnas.1210684109. PubMed.
9. Solcan N, Kwok J, Fowler PW, Cameron AD, Drew D, Iwata S, Newstead S. 2012. Alternating access mechanism in the POT family of oligopeptide transporters. *EMBO J* 31:3411–3421. 10.1038/emboj.2012.157. PubMed.
10. Ekici S, Yang H, Koch HG, Daldal F. 2012. Novel transporter required for biogenesis of cbb_3-type cytochrome *c* oxidase in *Rhodobacter capsulatus*. *mBio* 3:e00293-11. 10.1128/mBio.00293-11. PubMed.
11. Beaudoin J, Ekici S, Daldal F, Ait-Mohand S, Guerin B, Labbe S. 2013. Copper transport and regulation in *Schizosaccharomyces pombe*. *Biochem Soc Trans* 41:1679–1686. 10.1042/BST2013089. PubMed.
12. Ekici S, Turkarslan S, Pawlik G, Dancis A, Baliga NS, Koch HG, Daldal F. 2014. Intracytoplasmic copper homeostasis controls cytochrome *c* oxidase production. *mBio* 5:e01055-13. 10.1128/mBio.01055-13. PubMed.
13. Zhang Y, Blaby-Haas CE, Steimle S, Verissimo AF, Garcia-Angulo VA, Koch HG, Daldal F, Khalfaoui-Hassani B. 2019. Cu transport by the extended family of CcoA-like transporters (CalT) in proteobacteria. *Sci Rep* 9:1208. 10.1038/s41598-018-37988-4. PubMed.
14. Ekici S, Pawlik G, Lohmeyer E, Koch HG, Daldal F. 2012. Biogenesis of cbb_3-type cytochrome *c* oxidase in *Rhodobacter capsulatus*. *Biochim Biophys Acta* 1817:898–910. 10.1016/j.bbabio.2011.10.011. PubMed.

15. Khalfaoui-Hassani B, Wu H, Blaby-Haas CE, Zhang Y, Sandri F, Verissimo AF, Koch HG, Daldal F. 2018. Widespread distribution and functional specificity of the copper importer CcoA: distinct Cu uptake routes for bacterial cytochrome *c* oxidases. *mBio* 9:e00065-18. 10.1128/mBio.00065-18. PubMed.

16. Khalfaoui-Hassani B, Verissimo AF, Shroff NP, Ekici S, Trasnea P-I, Utz M, Koch HG, Daldal F. 2016. Biogenesis of cytochrome *c* complexes: from insertion of redox cofactors to assembly of different subunits, p 527–554. *In* Cramer WA, Kallas T (ed), Cytochrome complexes: evolution, structures, energy transduction and signaling. Springer, Dordrecht, the Netherlands.

17. Khalfaoui-Hassani B, Verissimo AF, Koch HG, Daldal F. 2016. Uncovering the transmembrane metal binding site of the novel bacterial major facilitator superfamily-type copper importer CcoA. *mBio* 7:e01981-15. 10.1128/mBio.01981-15. PubMed.

18. Dancis A, Yuan DS, Haile D, Askwith C, Eide D, Moehle C, Kaplan J, Klausner RD. 1994. Molecular characterization of a copper transport protein in *Saccharomyces cerevisiae*: an unexpected role for copper in iron transport. *Cell* 76:393–402. 10.1016/0092-8674(94)90345-X. PubMed.

19. Arguello JM, Patel SJ, Quintana J. 2016. Bacterial Cu^{+}-ATPases: models for molecular structure-function studies. *Metallomics* 8:906–914. 10.1039/c6mt00089d. PubMed.

20. Jiang J, Nadas IA, Kim MA, Franz KJ. 2005. A Mets motif peptide found in copper transport proteins selectively binds Cu(I) with methionine-only coordination. *Inorg Chem* 44:9787–9794. 10.1021/ic051180m. PubMed.

21. Taniguchi R, Kato HE, Font J, Deshpande CN, Wada M, Ito K, Ishitani R, Jormakka M, Nureki O. 2015. Outward- and inward-facing structures of a putative bacterial transition-metal transporter with homology to ferroportin. *Nat Commun* 6:8545. 10.1038/ncomms9545. PubMed.

22. Ke N, Berkmen M. 2014. Production of disulfide-bonded proteins in *Escherichia coli*. *Curr Protoc Mol Biol* 108:16.1B.1-21. 10.1002/0471142727.mb1601bs108. PubMed.

23. Verissimo AF, Khalfaoui-Hassani B, Hwang J, Steimle S, Selamoglu N, Sanders C, Khatchikian CE, Daldal F. 2017. The thioreduction component CcmG confers efficiency and the heme ligation component CcmH ensures stereo-specificity during cytochrome *c* maturation. *J Biol Chem* 292:13154–13167. 10.1074/jbc.M117.794586. PubMed.

24. Onder O, Verissimo AF, Khalfaoui-Hassani B, Peters A, Koch HG, Daldal F. 2017. Absence of thiol-disulfide oxidoreductase DsbA impairs cbb_3-type cytochrome *c* oxidase biogenesis in *Rhodobacter capsulatus*. *Front Microbiol* 8:2576. 10.3389/fmicb.2017.02576. PubMed.

25. De Feo CJ, Aller SG, Siluvai GS, Blackburn NJ, Unger VM. 2009. Three-dimensional structure of the human copper transporter hCTR1. *Proc Natl Acad Sci U S A* 106:4237–4242. 10.1073/pnas.0810286106. PubMed.

26. Puig S, Lee J, Lau M, Thiele DJ. 2002. Biochemical and genetic analyses of yeast and human high affinity copper transporters suggest a conserved mechanism for copper uptake. *J Biol Chem* 277:26021–26030. 10.1074/jbc.M202547200. PubMed.

27. Ren F, Logeman BL, Zhang X, Liu Y, Thiele DJ, Yuan P. 2019. X-ray structures of the high-affinity copper transporter Ctr1. *Nat Commun* 10:1386. 10.1038/s41467-019-09376-7. PubMed.

28. Long F, Su CC, Lei HT, Bolla JR, Do SV, Yu EW. 2012. Structure and mechanism of the tripartite CusCBA heavy-metal efflux complex. *Philos Trans R Soc Lond B Biol Sci* 367:1047–1058. 10.1098/rstb.2011.0203. PubMed.

29. Delmar JA, Su CC, Yu EW. 2015. Heavy metal transport by the CusCFBA efflux system. *Protein Sci* 24:1720–1736. 10.1002/pro.2764. PubMed.

30. Darrouzet E, Valkova-Valchanova M, Daldal F. 2002. The [2Fe-2S] cluster E(m) as an indicator of the iron-sulfur subunit position in the ubihydroquinone oxidation site of the cytochrome bc_1 complex. *J Biol Chem* 277:3464–3470. 10.1074/jbc.M107973200. PubMed.

31. Sambrook J, Russell DW. 2001. *Molecular cloning: a laboratory manual*, 3rd ed. Cold Spring Harbor Laboratory Press, Cold Spring Harbor, NY.

32. Laemmli UK. 1970. Cleavage of structural proteins during the assembly of the head of bacteriophage T4. *Nature* 227:680–685. 10.1038/227680a0. PubMed.

33. Koch HG, Winterstein C, Saribas AS, Alben JO, Daldal F. 2000. Roles of the ccoGHIS gene products in the biogenesis of the cbb_3-type cytochrome *c* oxidase. *J Mol Biol* 297:49–65. 10.1006/jmbi.2000.3555. PubMed.